CrossMark

CLINICAL STUDY

Distinctive localization and MRI features correlate of molecular subgroups in adult medulloblastoma

Fu Zhao[1,4] · Chunde Li[4] · Qiangyi Zhou[4] · Peiran Qu[2] · Bo Wang[4] · Xin Wang[2,4] ·
Shun Zhang[4] · Xingchao Wang[4] · Chi Zhao[1] · Jing Zhang[1] · Lin Luo[3] · Lin Ai[2] ·
Lei Xu[5] · Pinan Liu[1,4]

Abstract Medulloblastoma (MB) is recognized as comprising four molecular subgroups with distinct transcriptional profiles, clinical features, and outcomes. Previous studies demonstrate that pediatric MBs present with subgroup-specific MRI manifestations. We hypothesized that combination of anatomical localization and conventional features based on MR imaging can predict these subgroups in adult MBs. MR Imaging manifestations of 125 adult patients with MB were analyzed retrospectively based on pre-operative MRI scans. MB molecular subgroups were evaluated by the expression profiling array and immunohistochemistry. A pediatric MB cohort of 60 patients were analyzed for comparison with data of adult patients. Multiple logistic regression analysis revealed that tumor location ($P < 0.0001$) and pattern of enhancement ($P = 0.0048$) were significantly correlated with molecular subgroups in adult MBs. Ninety-two percent of adult MBs were correctly predicted by using logistic regression model based on the anatomical localization patterns and pattern of enhancement. Exclusively intra-cerebellar growth, localization in the rostral cerebellum, and no brainstem contact were specific to adult SHH-MBs. Group 4-MBs in adult were characterized by minimal/no enhancement compared with other two subgroups. Infant SHH-MBs represented significant different localization patterns compared with SHH tumors in children and adults. We identified that molecular subgroups of adult MBs could be well predicted by tumor localization patterns and enhancement pattern. Our study also provided important evidence that MB subgroups in adult possibly derived from different cellular origins.

Keywords Medullobalstoma · Adult · Localization · MRI · Molecular subgroup

✉ Fu Zhao
  zhaofu@bjctf.org

✉ Pinan Liu
  lpn@bjctf.org

1   Department of Neural Reconstruction, Beijing Neurosurgical Institute, Capital Medical University, Beijing, China

2   Department of Neuroimaging and Nuclear Medicine, Beijing Neurosurgical Institute, Capital Medical University, Beijing, China

3   Department of Neuropathology, Beijing Neurosurgical Institute, Capital Medical University, Beijing, China

4   Department of Neurosurgery, Beijing Tian Tan Hospital, Capital Medical University, No. 6 Tiantan Xili, Dongcheng District, Beijing, China

5   Department of Radiation Oncology, Massachusetts General Hospital and Harvard Medical School, Boston, MA, USA

Introduction

Medulloblastoma (MB) consists of four molecular subgroups (WNT, SHH, group 3, and group 4) with obvious differences in clinical outcomes. In pediatric patients, the WNT tumors have an excellent prognosis and should be treated with reduced radiation/chemotherapy, while Group 3-MBs and TP53-mutated SHH-MBs have worse outcome and need novel therapies [4, 8, 14, 18, 21, 27]. Because of the difference in response to therapy, tailored therapy for each subgroup is urgently needed. Additionally, MBs in adult show significantly different clinical features and outcomes in comparison to their pediatric counterparts [9, 13, 19, 26, 27]. In adult, Group 4-MBs are associated with worse

prognosis, while there is no significant difference between WNT and SHH-MBs [9, 19, 26].

The molecular classification of MB can provide important guidance to clinical treatment, however, it is not routinely used in the clinical practice to improve outcomes of patients. One of the reasons hampering its use is that the methods used for subgrouping require technical optimization: (i) gene expression profiling is widely used for MB subgroups analysis, while it is limited by the needs of high quality RNA and high cost [10, 15]; (ii) Immunostaining of several markers have been proposed to perform subgrouping, however, several challenges also remain in making immunohistochemistry (IHC) technique common to use in clinical, including variability in antibody batches, sample preparation methods, staining procedures, and inter-observer reliability [3, 14, 15].

Although imaging manifestations of MB are heterogeneous, recent studies demonstrate possible MRI features correlate for tumor subgroups in pediatric MBs, and may become a surrogate for genomic testing of classification [16, 17, 23, 25]. Considering its widespread use in clinical practice, MR imaging will be a convenient assisted approach if MB classification could be performed based on MRI. However, due to the low incidence, MRI features of adult MB are still not well described [1, 12], and whether the MR imaging also could be used to predict MB molecular subgroups in adult is still not known. Therefore, our study aimed to identify possible relation between MRI features and MB biology, and to reveal novel hints regarding the origins of MB subgroups in adult.

Patients and methods

Patient characteristics

A retrospective institutional data base search was conducted with institutional review board of Beijing Tian Tan Hospital approval and waiver of consent. All procedures performed in studies involving human participants were in accordance with the ethical standards of the institutional and/or national research committee and with the 1964 Helsinki declaration and its later amendments or comparable ethical standards. This article does not contain any studies with animals performed by any of the authors.

In this study, we retrospectively reviewed a cohort of 125 adult patients (male/female ratio 1.82:1; age range 18–60 years) with a final pathological diagnosis of MB from 2003 to 2016 at Beijing Tian Tan Hospital. Patients with both pre-operative MR imaging and surgical tissue available for molecular analysis were included. An independent pediatric cohort of 60 MBs (male/female ratio 2.07:1; age range 1.2–14 years) with the same with the same inclusion criteria was also assembled from Beijing Tian Tan Hospital.

Molecular analysis

In the adult cohort, expression profiling array (n = 13) and IHC (n = 112) were used to establish the MB molecular subgroups, as we described previously [26]. In the pediatric cohort, total RNA (100 ng) from fresh-frozen tissue was analyzed using the Panomics QuantiGene Plex 2.0 RNA assay system (Affymetrix, Santa Clara, CA, USA). Twenty-two MB subgroup-specific signature genes were selected for molecular classification analysis [10]. Two housekeeping genes (ACTB and GAPDH) were included for normalization. All of the experiments were performed following the user manual of QuantiGene Plex Assay (Panomics). Normalized expression ratios were generated by dividing the background-subtracted expression values by the geometric mean of the housekeeping genes. Unsupervised hierarchical cluster analysis was used to delineate distinct sample clusters.

Imaging technique and analysis

All patients were obtained brain MRI before surgery using 1.5 or 3T machine (Signa or Discovery 750; General Electric Medical Systems, Milwaukee, WI, USA). The following sequences were obtained including axial and coronal T2 FSE (TR/TE, 2700/100 ms), axial fluid-attenuated inversion recovery (TR/TE, 9000/120 ms; inversion time, 2200 ms), precontrast T1 spin-echo and contrast-enhanced T1 spoiled gradient-recalled echo (TR/TE, 8/3 ms; 1-mm section thickness, 0 skip), followed by 2 planes of contrast enhanced T1 spin-echo (TR/TE, 600–700/20 ms; 5 mm section thickness, 0.5 skip). Review and evaluation of the imaging data were reviewed independently by three experienced neuroradiologists (Q.P., X.Z., X.W.), who are blinded to clinical, pathologic, and molecular data. Consensus for discordant readings was decided chief neuroradiologists (L.A.).

Radiologic evaluation

Based on pre-operative MR imaging, tumor locations were defined as cerebellar hemisphere, midline vermis/4th ventricle or cerebellar peduncle/cerebellopontine angle cistern (CP/CPA). The anatomical localization patterns, presented in previous study [23], were described using spatial distribution with regard to four compartments: main tumor localization of hindbrain compartments, main localization in cerebellar compartments, main vertical localization in cerebellar compartments, and association with brainstem compartments.

The MR imaging features were analyzed including: tumor margin, enhancement characteristics, cysts/cavities, peritumoral edema, hemorrhage/mineralization, necrosis, tumor size and intracranial metastases. Tumor margin was

characterized as ill-defined if >50% of the margin could not be distinguished from the surrounding cerebellar parenchyma based on all imaging sequences. The enhancement pattern was defined as minimal/none if <10% was estimated to enhance, solid if enhancement was present in more than 90% of the tumor volume, heterogeneous if varying degrees of enhancement were seen in 10–90% of the tumor volume. The presence of hemorrhage/ mineralization was evaluated by gradient-echo MRI. When gradient-echo imaging was not available, CT scan was used to detect areas of hemorrhage/ mineralization.

Neurosurgical evaluation

Intraoperative diagnosis regarding primary tumor locations (cerebellar hemisphere, midline vermis/4th ventricle, or CP/CPA) and areas of brain invasion independently reviewed by four neurosurgeons (F.Z., B.W., X.W. and P.L.).

Statistical analysis

All statistical analyses were performed using statistics software (Statistical Package for the Social Sciences Statistics, Version 20.0; IBM, Armonk, New York) with an a priori significance level of P value = 0.01. Statistical analyses were performed by using the Fisher exact test, χ^2 test and Pearson correlation analysis for categoric data. A multivariable logistic regression model was developed to identify significant predictors of the MB subgroup. Pseudo R-squared goodness of fit ascertained by using the Cox and Snell method.

Results

Tumor staging, histology, and molecular subgroup

In this study, 125 adult MBs consisted of 17 WNT tumors (14%), 64 SHH tumors (51%), and 44 Subgroup 4 tumors (35%), and no subgroup 3-MB exited (Supplementary Fig. 1). SHH-MBs in adult occurred predominantly in the cerebellar hemispheres (69%, 44/64), while 22% (14/64) grew in midline vermis/4th ventricle, and 9% (6/64) were located the CP/CPA. WNT-MBs mainly located in midline vermis/4th ventricle (71%, 12/17), and 29% grew in CP/CPA (5/17). All Group 4-MBs (100%, 44/44) located at midline vermis/4th ventricle.

Sixty pediatric MBs were classified into four subgroups, including 8 WNT-MBs (13%), 17 SHH-MBs (28%), 15 Group 3-MBs (25%), and 20 Group 4-MBs (33%; Supplementary Fig. 2).

Anatomical localization patterns of adult MBs

We characterized anatomical localization patterns of 125 adult MBs using pre-operative MRI (Table 1). 69% of SHH-MBs showed exclusively intra-cerebellar growth and their overall distribution differed significantly from other two subgroups ($P < 0.0001$; Fig. 1c, d). Intracerebellar part only in hemisphere was characteristic of SHH tumors (40/64, 63%). In contrast, tumor parts affecting the cerebellum were mostly located in the vermis in the Group 4 tumors (36/44, 81%; Fig. 1e, f), while 47% WNT-MBs (8/17) were grew exclusively outside the cerebellum ($P < 0.0001$). Forty-eight percent of the SHH-MBs (31/61) burden exclusively in the rostral cerebellum (Fig. 1 c3, d3), but none of the other two subgroups had their main tumor burden exclusively in this localization ($P < 0.0001$). We further analyzed the association of MBs to different brainstem compartments. Interestingly, WNT-MBs and Group 4-MBs always had brainstem contact (Fig. 1a, b, e, f), and tumors mostly contacted both the cochlear and cuneate nucleus [75% (11/17) and 82% (36/44); respectively]. Conversely, only 25% (16/64) SHH-MBs had brainstem contact and mainly touched the cochlear nucleus ($P < 0.0001$).

Conventional MRI features of adult MBs

Conventional MRI features of molecular subgroup in adult are listed in Table 2. Group 4-MBs were characterized by minimal/none enhancement pattern (50%; $P < 0.0001$; Fig. 1f; Supplementary Fig. 4), compared with WNT- and SHH subgroups (0 and 9%; respectively). Cyst/cavities was predominately characteristic in WNT- and SHH-MBs (70 and 68%, respectively) groups, but not in Group 4-MBs (41%; $P = 0.008$). Meanwhile, 81% SHH-MBs and 53% WNT-MBs showed obvious peritumoral edema in cerebellum or brainstem (Fig. 1a–d), but only 36% Group 4 tumors had this feature ($P < 0.0001$). The other MR imaging features, including tumor margin, hemorrhage/ mineralization, size, or intracranial seeding, were not characteristic of specific molecular subgroups.

Models for determining molecular subgroups of adult MBs

Multivariable logistic regression showed that locations (midline vermis/4th ventricle, cerebellar hemisphere and CP/CPA, $P < 0.0001$) and pattern of enhancement ($P = 0.0048$) were predictors of adult MB subgroups. Two logistic regression models based on different MR imaging patterns were used for determining molecular subgroups. With the logistic regression model based on location and pattern of enhancement, 79% of tumors were appropriately classified, including WNT-MBs (24%), SHH-MBs

Table 1 Tumor localization of molecular subgroups in adult medulloblastoma

Localization	WNT (n = 17) No. of patients (%)	SHH (n = 64) No. of patients (%)	Group 4 (n = 44) No. of Patients (%)	P (χ^2)
Intra-/extra-cerebellar				3.72e−20
Only intra-cerebellar	0 (0.0)	44 (68.8)	0 (0.0)	
Intra- + extra-cerebellar	9 (52.9)	20 (31.2)	39 (88.6)	
Only extra-cerebellar	8 (47.1)	0 (0.0)	5 (11.4)	
Horizontal localization in Cb				6.29e−19
Vermis & hemisphere	3 (17.6)	13 (20.3)	5 (11.4)	
Vermis	2 (11.8)	11 (17.2)	34 (77.3)	
Hemisphere	4 (23.5)	40 (62.5)	0 (0.0)	
Extra-cerebellar	8 (47.1)	0 (0.0)	5 (11.4)	
Vertical localization in Cb				1.17e−14
Caudal	1 (5.8)	0 (0.0)	5 (11.4)	
Rostral	0 (0.0)	31 (48.4)	0 (0.0)	
Rostro-caudal	8 (47.1)	33 (51.6)	34 (77.3)	
Extra-cerebellar	8 (47.1)	0 (0.0)	5 (11.4)	
BS contact				2.07e−28
BS other localization only	0 (0.0)	5 (7.8)	0 (0.0)	
Ncl. cochlear + cuneate	11 (64.7)	3 (4.7)	36 (81.8)	
Ncl. cuneate	0 (0.0)	0 (0.0)	8 (18.2)	
Ncl. cochlear	6 (35.3)	13 (20.3)	0 (0.0)	
No BS contact	0 (0.0)	43 (67.2)	0 (0.0)	

BS brainstem, *Ncl* nucleus, *Cb* cerebellum

(86%) and Group 4-MBs (91%). This multivariable model demonstrated a goodness of fit as assessed by the pseudo R-squared goodness of fit (Cox and Snell method) of 0.669. With the logistic regression model based on anatomical localization patterns and pattern of enhancement, 92% of tumors were appropriately classified (Supplementary Fig. 3), including WNT-MBs (65%), SHH-MBs (95%) and Group 4-MBs (98%). The multivariable model demonstrated a goodness of fit as assessed by the pseudo R-squared goodness of fit (Cox and Snell method) of 0.795.

Neurosurgical findings in adult MBs

Surgical inspection regarding the tumor location was 100% concordant with the pre-operative MR imaging result. All Group 4-MBs (44/44) and 76% WNT-MBs (13/17) expanded into the fourth ventricle, whereas only 8% SHH-MBs (5/64) grew intraventricularly ($P < 0.0001$). Meanwhile, 76% WNT-MBs (13/17) were found obviously adherent to the 4th ventricle floor at surgery, compared with only 34% for Group-4 MBs (15/44) and none for SHH-MBs ($P < 0.0001$). Interestingly, 59% WNT-MBs (10/17) were found expanded into the foramen of Luschka, but only 30% Group-4 MBs (13/44) and none for SHH-MBs had the foramen of Luschka involved ($P < 0.0001$).

Anatomical localization patterns and conventional features of pediatric MBs

In the pediatric cohort, SHH-, WNT- and Group 4-MBs also had significantly different distribution on each localization pattern ($P < 0.01$, respectively; Supplementary Table 1). Of all various conventional MRI features, Group 4-MBs were also characterized by minimal/none enhancement pattern (60%) compared with two other subgroups ($P < 0.0001$, Supplementary table 2). The other MR imaging features were not characteristic of specific molecular subgroups in this cohort.

Comparison of localization patterns and features between adult and pediatric MBs

Attributed to the same subgroup, there was no significant difference of localization patterns or conventional features between adult and pediatric MBs (Supplementary Table 3–8). Notably, SHH-MBs in infants, children, and adults represented distinct anatomical localization obviously (Table 3). Most SHH-MBs in children and adults showed exclusively intra-cerebellar growth (68, 69%; respectively), while only 13% infant SHH-MBs (1/8) grew totally inside the cerebellum ($P = 0.002$). As the tumor parts affecting the cerebellum, SHH-MBs in children and adults always located in the hemispheres (56 and 63%; respectively).

Fig. 1 Exemplary MRIs of MBs in adult from the three molecular subgroups (T1-weighted post-contrast axial, sagittal and coronal MRIs). **a**1-3, A WNT tumor in the CP/CPA region is shown. **b**1-3, An intraventricular WNT-MB with bilateral brainstem contact is shown. **c**1-3, A SHH tumor located in the cerebellar hemispheres is shown. **d**1-3, A SHH tumor located in caudal vermis is shown. **e**1-3, A Group 4 tumor located in the midline fourth ventricle with minimal/no enhancement is shown. **f**1-3, An intraventricular Group 4 tumor is shown (*Inset*: tuber vermis involved)
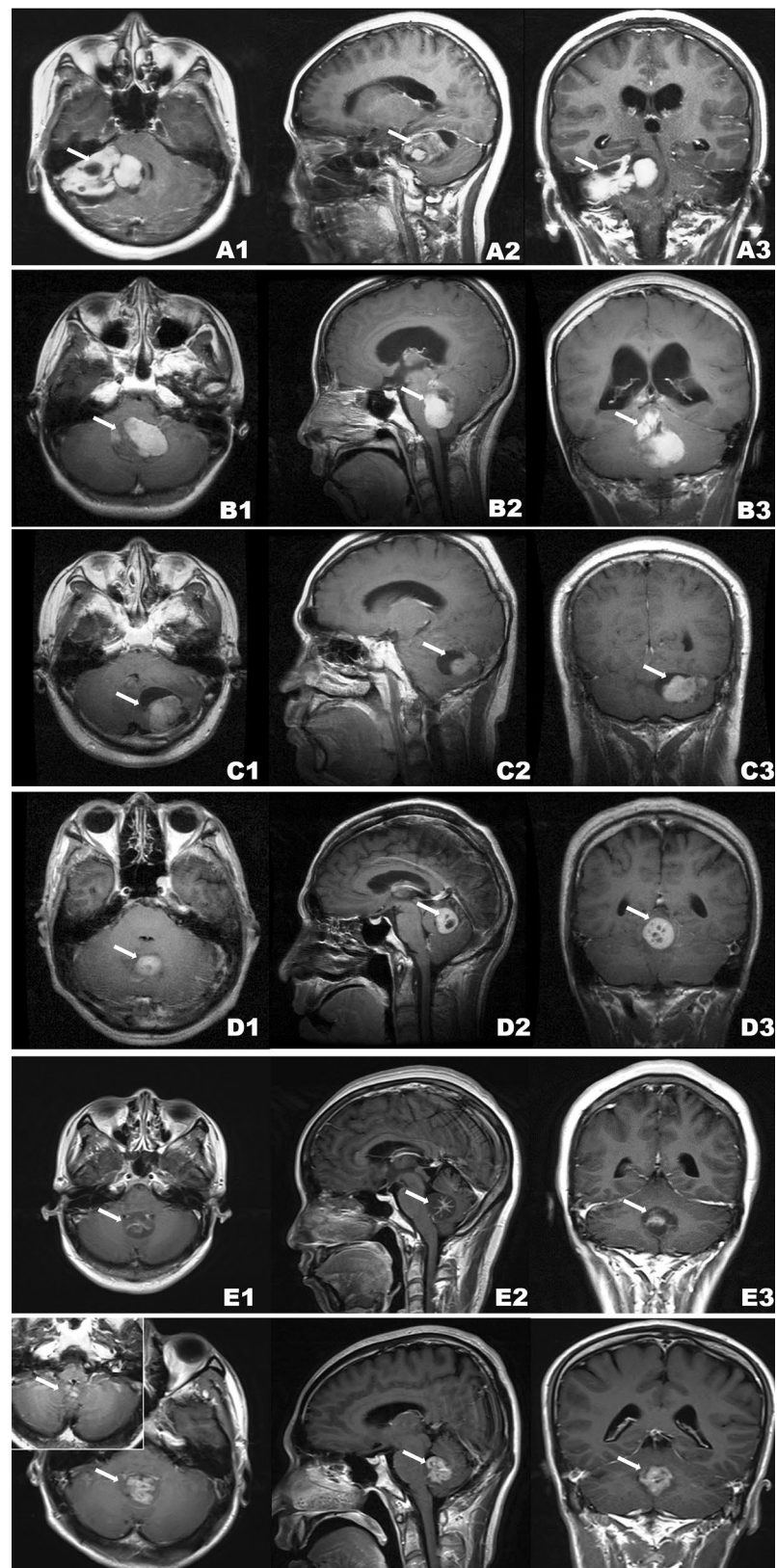
Table 2 MRI features of three molecular subgroups in adult medulloblastoma

Characteristic	WNT (n = 17)	SHH (n = 64)	Group 4 (n = 44)	$P(\chi^2)$
	No. of patients (%)	No. of patients (%)	No. of Patients (%)	
Enhancement pattern				9.64e−07
Minimal/none	0 (0.0)	6 (9.4)	22 (50.0)	
Heterogeneous	14 (82.4)	40 (62.5)	21 (45.5)	
Solid	3 (17.6)	18 (28.1)	2 (4.5)	
Cysts/ cavities				0.008
Yes	12 (70.6)	44 (68.8)	18 (40.9)	
No	5 (29.4)	20 (31.3)	26 (59.1)	
Peritumoral edema				4.2e−05
Yes	9 (52.9)	52 (81.3)	16 (36.4)	
No	8 (47.1)	12 (18.8)	28 (63.6)	
Ill-defined margins				0.065
Yes	3 (17.6)	16 (25.0)	19 (43.2)	
No	14 (82.4)	48 (75.0)	25 (56.8)	
Necrosis				0.186
Yes	10 (58.8)	22 (34.4)	12 (27.3)	
No	7 (41.2)	42 (65.6)	32 (72.7)	
Hemorrhage/mineralization				0.965
Yes	11 (64.7)	40 (62.5)	29 (65.9)	
No	6 (35.3)	24 (37.5)	15 (34.1)	
Seeding				0.057
Yes	2 (11.8)	2 (3.1)	7 (15.9)	
No	15 (88.2)	62 (96.9)	37 (84.1)	

Table 3 The comparison of tumor localization among infant, childhood, and adult SHH-MB

Localization	Infant (n = 8)	Children (n = 9)	Adult (n = 64)	$P(\chi^2)$
	No. of patients (%)	No. of Patients (%)	No. of patients (%)	
Intra-/extra-cerebellar				0.002
Only intra-cerebellar	1 (12.5)	7 (66.7)	44 (68.8)	
Intra- + extra-cerebellar	6 (75.0)	2 (33.3)	20 (31.2)	
Only extra-cerebellar	1 (12.5)	0 (0.0)	0 (0.0)	
Horizontal localization in Cb				0.004
Vermis & hemisphere	2 (25.0)	4 (44.4)	13 (20.3)	
Vermis	4 (50.0)	0 (0.0)	11 (17.2)	
Hemisphere	1 (12.5)	5 (55.6)	40 (62.5)	
Extra-cerebellar	1 (12.5)	0 (0.0)	0 (0.0)	
Vertical localization in Cb				0.036
Caudal	0 (0.0)	0 (0.0)	0 (0.0)	
Rostral	1 (12.5)	3 (33.3)	30 (46.9)	
Rostro-caudal	6 (75.0)	6 (66.7)	34 (53.1)	
Extra-cerebellar	1 (12.5)	0 (0.0)	0 (0.0)	
BS contact				0.066
BS other localization only	0 (0.0)	0 (0.0)	5 (7.8)	
Ncl. cochlear + cuneate	3 (37.5)	1 (11.1)	3 (4.7)	
Ncl. cuneate	0 (0.0)	0 (0.0)	0 (0.0)	
Ncl. cochlear	2 (25.0)	1 (11.1)	13 (20.3)	
No BS contact	3 (37.5)	7 (77.8)	43 (67.2)	

BS brainstem, *Ncl* nucleus, *Cb* cerebellum

Contrarily, 50% of infant SHH-MBs (4/8) located in the vermis ($P = 0.004$). Moreover, SHH-MBs in elder patients tended to present more often located only in the rostral cerebellum compared with infant SHH-MBs ($P = 0.036$). In addition, there was no significant difference of MRI features among three age groups. (Supplementary Table 9).

Discussion

Previous studies in pediatric MBs have demonstrated that different molecular subgroups present with specific imaging features [16, 17, 23, 25]. Meanwhile, MR imaging study could provide significant insights to the precise cells of origin of human MB, which have already shown distinctive developmental origins of MB molecular subgroups in mice [5, 6, 20, 24]. However, due to the rare occurrence, little is known about the relationship between molecular subgroups and imaging characteristics of adult MBs. To fill the gap, we represent the first and largest study, to investigate subgroup-specific localization and MRI features in adult MBs. Our results demonstrate that most of adult MB subgroups could be well distinguished by anatomic localization patterns and pattern of enhancement based on MRI.

SHH-MBs in adult present with distinctive localization from WNT- and Group 4-MBs. In our study, most SHH-MBs presented with exclusive intracerebellar growth, especially with the cerebellar hemisphere involvement. This MRI-based specific localization can be a significant predictor for adult SHH-MB (Supplementary Fig. 3). Furthermore, we suggest that a majority of adult SHH-MBs may derive from intra-cerebellar origins as they may appear without any growth out the cerebellum. Our finding may also support the prior study that the third population of stem/precursor cells—white matter stem cells may be cells of origin of some adult MBs [11]. Moreover, all of adult SHH-MBs grew in the rostral or rostro-caudal cerebellum, but this was never the case in WNT- or Group 4 MBs. These specific localization patterns evaluate that adult SHH-MBs are distinct tumors from other two subgroups and likely have a different cell of origin. These results also confirm previous studies that granule neuron precursor cells (GNPCs) derived from the upper rhombic lip formed SHH-MBs in mice [20, 24].

The spatial distribution of WNT-MBs is heterogeneous and still controversial in pediatric MBs. Previous studies described that all of pediatric WNT-MBs locate in the midline [5, 22]. Conversely, two recent reports demonstrated that WNT tumors mainly occurred along the CP/CPA (50, 75%) [16, 17]. In our cohort, most of adult WNT-MBs and all pediatric WNT-MBs grew in the middle line, only 30% adult WNT-MBs located at CP/CPA. The common characteristic of all WNT-MBs in our study was brainstem involvement. This finding can provide the potential evidence that brainstem precursors could be cells of origin for WNT-MBs. In addition, we also found 9% adult SHH-MBs located in CP/CPA. Most of them could be distinguish from CP/CPA WNT tumors with characteristic of the caudal-cerebellum growth.

The origin of Group 4-MBs are less well characterized because of its unclear molecular pathogenesis and lack of appropriate animal models to study. Interestingly, the localization of Group 4-MBs in adult showed remarkable consistency (Supplementary Fig. 4). All Group 4 tumors grew into the 4th ventricle with both the cochlear and cuneate nucleus contact. Meanwhile, most of Group 4 tumors occured in specific site with involvement of inferior vermis and cisterna magna. Therefore, we hypothesis that the cell of origin for Group 4-MBs in adult possibly originate from superficial layer cells of tuber vermis or inferior medullary velum (Supplementary Fig. 5). In addition, we found that Group 4 tumors in adult present with minimal/no enhancement and less intratumoral cysts on MR imaging, compared with other two subgroups. Based on these, we conclude that minimal/no enhancing tumors with both the cochlear and cuneate nucleus contact can be well recognized as Group 4 subgroups (Supplementary Fig. 3).

Our study also included a pediatric cohort to make valid comparisons between adult and pediatric patients. Although localization and features based on MRI were similar between adult and pediatric MBs attributed to the same subgroups, the significant differences of localization pattern were found in age-related SHH-MBs. Infant SHH-MBs always grew in vermis and expanded into 4th ventricle, which were particularly specific from SHH-MBs in old patients (>3 years old). Furthermore, the childhood and adult SHH-MBs were more often located in rostral cerebellum than infant SHH-MBs. Since most SHH tumors occur in infant and adult patients, our finding proved that adult SHH-MBs are totally different from infant SHH-MBs with characteristic localization and distinct cellular origin. Previous studies prove that SHH-MBs are gnomically distinct in infants, children, and adults [2, 7, 13]. Recent study identifies four different subtypes of SHH MB across different age groups have disparate biology and outcomes [2]. Thus, we suggest that different therapeutic strategy for adult SHH-MBs are needed in future clinical trials and may have the potential for clinical benefit.

Future large-scaled, multi-centered retrospective studies are needed to further confirm our study, and the tumor size should be within a set limit to accurately correlate with anatomical localization. A second limitation of our study is that the molecular-subgroup were classified by immunohistochemistry. To overcome this limitation, future studies using fresh frozen tumor tissues followed by real-time PCR assay or nanoString assay for molecular analysis are needed [10, 15]. In addition, adult Group 3-MBs are not included in this study because of rare incidence [8, 19, 26]. The imaging

features of this subgroup in adult are still unknown, and need to be analyzed in future studies.

In conclusion, our data identified the specific localization and MRI features of MB subgroups in adult, and provided evidence for profound implications regarding the different cellular origin. As to be the widespread non-invasive method for clinical diagnosis in brain tumors, MR imaging correlates of each MB subgroup will undoubtedly improve benefits of translating molecular classification into clinical arena for prognostic evaluation.

Author contributions Conception and design—FZ, LA, LL, LX, PL; Provision of study materials and/or patients—LC, BW; Collection and assembly of data—PL, JZ, PQ, QZ; Data analysis and interpretation—ZF, LC, XW; CZ; XW; Manuscript writing—All authors; Final approval of manuscript—All authors.

Compliance with ethical standards

Conflict of interest The authors declare that they have no conflict of interest.

References

1. Bourgouin PM, Tampieri D, Grahovac SZ et al (1992) CT and MR imaging findings in adults with cerebellar medulloblastoma: comparison with findings in children. AJR Am J Roentgenol 159:609–612. doi:10.2214/ajr.159.3.1503035

2. Cavalli FMG, Remke M, Rampasek L et al (2017) Intertumoral heterogeneity within medulloblastoma subgroups. Cancer Cell 31(737–754):e736. doi:10.1016/j.ccell.2017.05.005

3. Ellison DW, Dalton J, Kocak M et al (2011) Medulloblastoma: clinicopathological correlates of SHH, WNT, and non-SHH/WNT molecular subgroups. Acta Neuropathol 121:381–396. doi:10.1007/s00401-011-0800-8

4. Ellison DW, Kocak M, Dalton J et al (2011) Definition of disease-risk stratification groups in childhood medulloblastoma using combined clinical, pathologic, and molecular variables. J Clin Oncol 29:1400–1407. doi:10.1200/JCO.2010.30.2810

5. Gibson P, Tong Y, Robinson G et al (2010) Subtypes of medulloblastoma have distinct developmental origins. Nature 468:1095–1099. doi:10.1038/nature09587

6. Grammel D, Warmuth-Metz M, von Bueren AO et al (2012) Sonic hedgehog-associated medulloblastoma arising from the cochlear nuclei of the brainstem. Acta Neuropathol 123:601–614. doi:10.1007/s00401-012-0961-0

7. Kool M, Jones DT, Jager N et al (2014) Genome sequencing of SHH medulloblastoma predicts genotype-related response to smoothened inhibition. Cancer Cell 25:393–405. doi:10.1016/j.ccr.2014.02.004

8. Kool M, Korshunov A, Remke M et al (2012) Molecular subgroups of medulloblastoma: an international meta-analysis of transcriptome, genetic aberrations, and clinical data of WNT, SHH, Group 3, and Group 4 medulloblastomas. Acta Neuropathol 123:473–484. doi:10.1007/s00401-012-0958-8

9. Korshunov A, Remke M, Werft W et al (2010) Adult and pediatric medulloblastomas are genetically distinct and require different algorithms for molecular risk stratification. J Clin Oncol 28:3054–3060. doi:10.1200/JCO.2009.25.7121

10. Kunder R, Jalali R, Sridhar E et al (2013) Real-time PCR assay based on the differential expression of microRNAs and protein-coding genes for molecular classification of formalin-fixed paraffin embedded medulloblastomas. Neuro Oncol 15:1644–1651. doi:10.1093/neuonc/not123

11. Lee A, Kessler JD, Read TA et al (2005) Isolation of neural stem cells from the postnatal cerebellum. Nat Neurosci 8:723–729. doi:10.1038/nn1473

12. Malheiros SM, Carrete H Jr, Stavale JN et al (2003) MRI of medulloblastoma in adults. Neuroradiology 45:463–467. doi:10.1007/s00234-003-1011-3

13. Northcott PA, Hielscher T, Dubuc A et al (2011) Pediatric and adult sonic hedgehog medulloblastomas are clinically and molecularly distinct. Acta Neuropathol 122:231–240. doi:10.1007/s00401-011-0846-7

14. Northcott PA, Korshunov A, Witt H et al (2011) Medulloblastoma comprises four distinct molecular variants. J Clin Oncol 29:1408–1414. doi:10.1200/JCO.2009.27.4324

15. Northcott PA, Shih DJ, Remke M et al (2012) Rapid, reliable, and reproducible molecular sub-grouping of clinical medulloblastoma samples. Acta Neuropathol 123:615–626. doi:10.1007/s00401-011-0899-7

16. Patay Z, DeSain LA, Hwang SN et al (2015) MR imaging characteristics of wingless-type-subgroup pediatric medulloblastoma. AJNR Am J Neuroradiol 36:2386–2393. doi:10.3174/ajnr.A4495

17. Perreault S, Ramaswamy V, Achrol AS et al (2014) MRI surrogates for molecular subgroups of medulloblastoma. AJNR Am J Neuroradiol 35:1263–1269. doi:10.3174/ajnr.A3990

18. Ramaswamy V, Remke M, Bouffet E et al (2013) Recurrence patterns across medulloblastoma subgroups: an integrated clinical and molecular analysis. Lancet Oncol 14:1200–1207. doi:10.1016/S1470-2045(13)70449-2

19. Remke M, Hielscher T, Northcott PA et al (2011) Adult medulloblastoma comprises three major molecular variants. J Clin Oncol 29:2717–2723. doi:10.1200/JCO.2011.34.9373

20. Schuller U, Heine VM, Mao J et al (2008) Acquisition of granule neuron precursor identity is a critical determinant of progenitor cell competence to form Shh-induced medulloblastoma. Cancer Cell 14:123–134. doi:10.1016/j.ccr.2008.07.005

21. Taylor MD, Northcott PA, Korshunov A et al (2012) Molecular subgroups of medulloblastoma: the current consensus. Acta Neuropathol 123:465–472. doi:10.1007/s00401-011-0922-z

22. Teo WY, Shen J, Su JM et al (2013) Implications of tumor location on subtypes of medulloblastoma. Pediatr Blood Cancer 60:1408–1410. doi:10.1002/pbc.24511

23. Wefers AK, Warmuth-Metz M, Poschl J et al (2014) Subgroup-specific localization of human medulloblastoma based on pre-operative MRI. Acta Neuropathol 127:931–933. doi:10.1007/s00401-014-1271-5

24. Yang ZJ, Ellis T, Markant SL et al (2008) Medulloblastoma can be initiated by deletion of Patched in lineage-restricted progenitors or stem cells. Cancer Cell 14:135–145. doi:10.1016/j.ccr.2008.07.003

25. Yeom KW, Mobley BC, Lober RM et al (2013) Distinctive MRI features of pediatric medulloblastoma subtypes. AJR Am J Roentgenol 200:895–903. doi:10.2214/AJR.12.9249

26. Zhao F, Ohgaki H, Xu L et al (2016) Molecular subgroups of adult medulloblastoma: a long-term single-institution study. Neuro Oncol 18:982–990. doi:10.1093/neuonc/now050

27. Zhukova N, Ramaswamy V, Remke M et al (2013) Subgroup-specific prognostic implications of TP53 mutation in medulloblastoma. J Clin Oncol 31:2927–2935. doi:10.1200/JCO.2012.48.5052